PAPER

Simple planar Hall effect based sensors for low-magnetic field detection

To cite this article: Le Khac Quynh *et al* 2019 *Adv. Nat. Sci: Nanosci. Nanotechnol.* **10** 025002

Simple planar Hall effect based sensors for low-magnetic field detection

Le Khac Quynh[1,2], Nguyen The Hien[1], Nguyen Hai Binh[3], Tran Tien Dung[2], Bui Dinh Tu[1], Nguyen Huu Duc[1] and Do Thi Huong Giang[1]

[1] Faculty of Engineering Physics and Nanotechnology, University of Engineering and Technology, Vietnam National University Hanoi, 144 Xuan Thuy Road, Hanoi, Vietnam
[2] Faculty of Physics, Ha Noi Pedagogical University 2, 32 Nguyen Van Linh Road, Xuan Hoa, Phuc Yen, Vinh Phuc, Vietnam
[3] Institute of Materials Science, Vietnam Academy of Science and Technology, 18 Hoang Quoc Viet Road, Hanoi, Vietnam

E-mail: quynhlk@gmail.com

Abstract

Magnetic field sensors based on the planar Hall effect using single layer $Ni_{80}Fe_{20}$ thin films have been designed, fabricated and characterized. By optimizing the sensor's dimension, such as the thickness and the length to width ratio, experimental results have shown that the sensor's sensitivity could be increased up to three times thanks to the enhancement of the shape magnetic anisotropy. The highest sensitivity of $100\,\mu V\,Oe^{-1}$ corresponding to the relative resistance change up to $20\,m\Omega/Oe$ was achieved at a supplied DC current of 5 mA for the cross-shaped geometry of the sensor with 5 nm in the thickness and a length/width ratio of 10. Simple structure, low fabrication cost, and low power consumption make this sensor very promising for low field magnetic field sensing such as geomagnetic field detections.

Keywords: planar Hall effect, magnetic sensor, anisotropic magnetoresistance effect (AMR), permalloy

Classification numbers: 2.00, 4.10, 4.13, 4.14

1. Introduction

The planar Hall effect (PHE), also known as the anisotropic magnetoresistance (AMR) effect, presents the material's resistivity change due to an external magnetic field. Besides other factors, the scale of this effect depends on the angle between the vector of the current density j and the magnetization M [1]. The PHE has been widely utilized in the development of various types of high performance magnetic field sensors, including those based on spin valves (SV), giant magnetoresistance (GMR), tunnelling magnetoresistance (TMR) etc [2–13]. While PHE-based magnetic sensors are currently widely utilized in detection of magnetic flux leakage, magnetic particles and in the development of biosensors for biological and biomedical application [14–18], the sensors based on the electromagnetic effect and AMR effect are more preferably applied for magnetic field sensing and measurements, especially the Earth's magnetic field [9, 19–21]. In

order to study the application of PHE sensors for the Earth's magnetic field measurement, it is important to evaluate their sensitivity in the low magnetic field region.

In numerous studies of the PHE in multilayer structures of NiFe/IrMn, NiFe/Cu/NiFe, NiFe/Cu/NiFe/IrMn etc to develop Hall sensors for magnetic field measurements, such cross-shaped ones have been found to exhibit the maximum sensitivity of $19.86\,\mu V/Oe$ [4, 12, 16]. Figure 1 below presents the structure and the functional principle of a cross-shaped sensor [1].

In this arrangement, when the current j flows along the x-axis of the sensor, the output voltage V_y in the y-direction perpendicular to the x-axis is given by the expression [1, 12]:

$$V_y = I_x \Delta R \sin \theta \cos \theta \qquad (1)$$

with $\Delta R = (\rho_\parallel - \rho_\perp)/t$, where t is the thickness of the thin film, $\rho_\parallel$ and $\rho_\perp$ are the electrical resistivity measured with the current parallel and perpendicular to the easy magnetization
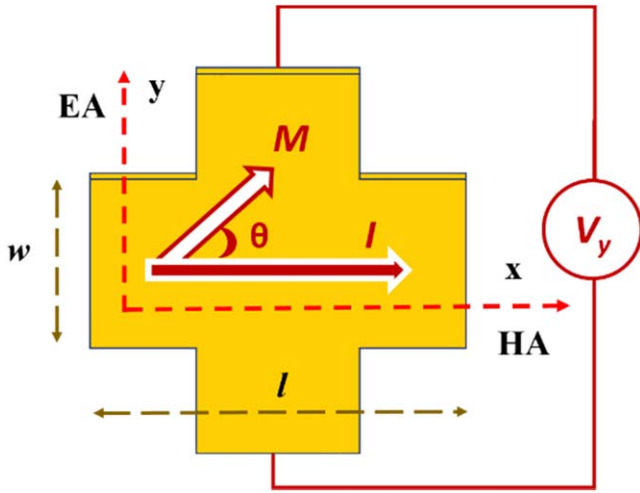
Figure 1. Structure and function of a PHE based cross-shaped sensor.

axis of the sample, respectively, and θ is the angle between the magnetization vector and the current flow.

For small θ angles, the PHE voltage exhibits a linear and highly sensitive field response in the low field region (*i.e.* $H < 50$ Oe). In this case, the PHE output voltage and the sensitivity of the sensor are given as [1, 12]:

$$V_y = I_x \Delta R \sin \theta \approx I \Delta R \frac{H_{app}}{H_K}, \tag{2}$$

$$S = \frac{\Delta R}{H_K}, \tag{3}$$

where $H_K = 2K/M_S$ is the anisotropy field with K as the anisotropy constant, M_S as the saturation magnetization. K and M_S both depend on the magnetic anisotropy and the thickness of the sensor (For NiFe thin films, K and M_S are about 2 kerg/cm^3, 800 emu cm^{-3}, respectively [12]).

Furthermore, Henriksen [2, 5] have reported that the sensitivity of Hall sensors could become about 100 times greater when these are arranged in a Wheatstone bridge configuration. Dau *et al* [15] found that a PHE sensor using single NiFe layers could also reduce the thermal drift which is the main source of noise, by at least four orders of magnitude. These results suggest that this type of cross-shape PHE sensors can be used to efficiently detect weak magnetic fields in the nano-tesla range [15].

In the research group of the Vietnam National University (VNU)-Key Laboratory for Micro-Nano Technology at the University of Engineering and Technology (UET), there have been some significant progresses achieved in the development of these cross-shaped types of sensors [1, 4]. Optimally, simplifying the fabrication procedure to significantly reduce the manufacturing costs of the sensors while satisfactorily meeting the highly sophisticated requirements of detection and measurement of low magnetic fields toward the commercialization of the product would be some urgent issues of current concerns. In this work, we report an approach of developing a planar Hall effect cross-shaped sensor using soft magnetic Ni$_{80}$Fe$_{20}$ single layer thin films for the highly efficient detection and measurement of low magnetic fields. We will focus on the enhancement of the magnetic sensitivity of the NiFe thin film based planar Hall effect sensors, especially at low magnetic fields. The measures include (i) the optimization of the sensor's dimension (via the ratio of the length (L) to the width (W) of the sensor), (ii) the optimization of the pinning magnetic field (H_{bias}) of the NiFe thin film and (iii) the optimization of the NiFe thin film thickness toward the sensor's output signal. The governing idea is strengthening the uniaxial magnetic anisotropy thanks to the shape magnetic anisotropy enhancement along the pinned direction.
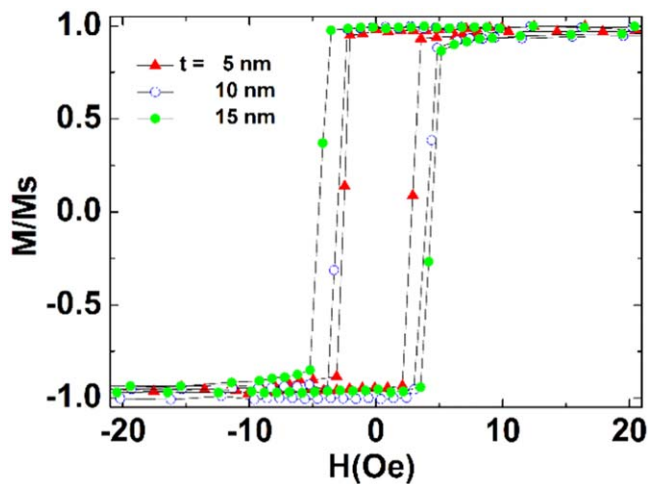
2. Experiments

A cross-shaped sensor consists of two same resistor bars in orthogonal geometry. In this study, sensors of different sizes, including 1×5, 1×7 and 1×10 mm^2 (in width and length), and with different NiFe film thicknesses of 5, 10 and 15 nm were fabricated. The polymer masks were first made by the lithography technology using a lithograph of the Model MJB4 (Suss Microtec, Germany) and the sensors were then magnetron sputtered using the sputter of the Model ATC-2000F (AJA International Inc., USA) at the VNU Key Laboratory for Micro-Nano Technology at the UET. The electrodes of the sensors were made of Cu, also by sputtering. The procedure for the fabrication of the sensors is the same as described in previous works [8, 22] and illustrated in figure 2.

The measurements of the characteristics of the synthesized materials and the fabricated sensors were conducted on
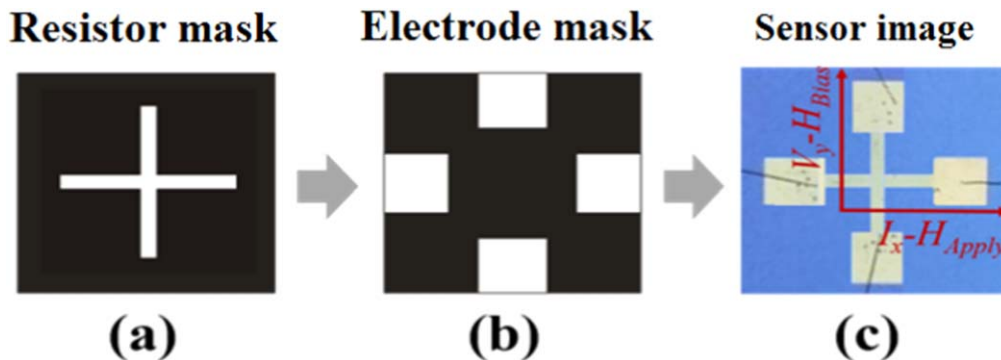
Figure 2. Fabrication process and the structure of the complete sensor: (a) Resistor mask, (b) Electrode mask and (c) Image of fabricated sensor.

Figure 3. Magnetic hysteresis loops of the NiFe films measured in the external magnetic field applied along the pinning field direction (H_{bias}) (t = 5, 10, 15 nm).

Figure 4. Magnetic hysteresis loops of NiFe films in different pinning magnetic fields (H_{bias}).

the experimental setups used in our previous works [8, 22]. It is, however, noteworthy here that the output voltage of the sensor was recorded at room temperature by a Keithley 2000 Multimeter, using the Keithley 6220 DC Precision Current Source.

During the sputtering process, a pinning magnetic field (H_{bias}) of 900 Oe is applied parallel to the *y*-axis of the cross-shaped sensor mask (denoted as easy axis (EA)). The pinning field was provided by two parallel magnet bars attached to the substrate holder, helping to form the easy magnetization axis of the sensor. Under the applied magnetic fields, the change of the resistance on the resistor bars due to the Hall effect will correspondingly cause the changes in the sensor output voltage (V_y). This indeed is also the function principle of the cross-shaped sensors. To study the sensor's performance, a current of I_x and an external magnetic field H_{app} were applied along the *x*-axis, which is the hard axis (HA) of the sensor, *i.e.* perpendicular to the EA axis. This external magnetic field H_{app} was provided by a Helmholtz coil [8, 22]. The measured output voltage of the sensor is then dependent on the applied magnetic field both in strength and orientation.

3. Results and discussions

3.1. Characterization of the magnetic properties of the NiFe thin films

From the fabrication process described in the previous section, the sensor is of uniaxial magnetic anisotropy with the anisotropy axis oriented along the pinning magnetic field that is applied parallel to the *y*-axis of the sensor (see figure 2(c) above). To characterize the magnetic nature of the NiFe thin films, the same sample's size of $10 \times 10 \text{ mm}^2$ and different thicknesses of 5, 10 and 15 nm were sputtered on glass substrates. Magnetic hysteresis loops were measured on these films with the measuring magnetic field applied parallel to the EA of the film and the results are presented in figure 3. From
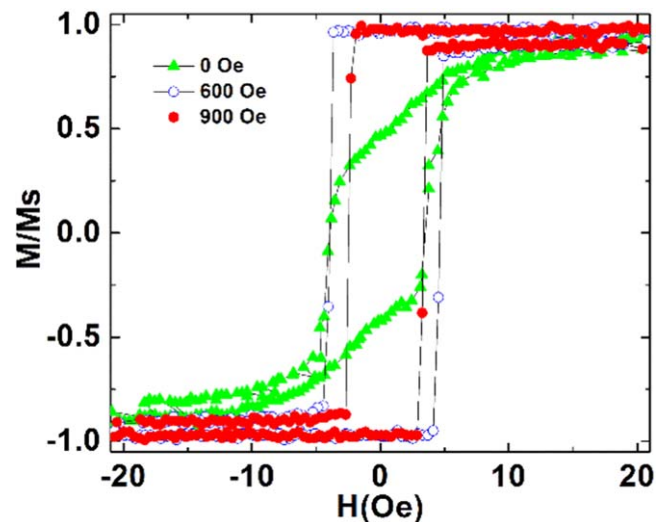
these results, a coercive field of $H_c \leqslant 6$ Oe has been derived for all of the thin films indicating the as-prepared NiFe thin films to be of soft magnetic nature. It is also clearly seen that the thinner NiFe film was, the lower coercivity was obtained. This soft magnetic behavior suggests that the thinner films shall induce higher response signals in the low magnetic field regions. As it is seen, the coercivity of the NiFe film with thickness of 5 nm is only of 2.2 Oe, which is 1.8 and 2.4 times smaller than that of the NiFe film with respective thicknesses of 10 and 15 nm. The measured results also reveals an increase of the anisotropy field H_K with the increasing film thickness, namely H_K = 9.2 Oe for the 5 nm thick NiFe film, H_K = 17.6 Oe for the 10 nm film and H_K = 22.9 Oe for the 15 nm one. According to equation (3) above, the 5 nm thick film will provide the highest sensitivity. Based on these findings, the NiFe film thickness of t = 5 nm is considered as efficient in all of sensor geometric configurations concerned in this study.

We have studied the magnetization of the NiFe thin film in the presence of the external magnetic fields where three different values of the pinning magnetic field were applied, namely H_{bias} = 900, 600 and 0 Oe. Magnetic hysteresis loops of the NiFe films were recorded along the easy magnetization direction and results are shown in figure 4. The magnetization loop becomes almost rectangular in the presence of the pinning fields. Among them, the sample with H_{bias} = 900 Oe reveals the best magnetic softness with the lowest magnetic coercive field. This means that the NiFe thin film prepared with the pinning field of 900 Oe exhibits the best uniaxial magnetic anisotropy with an anisotropy field of about 10 Oe, consistent with the reported value [22]. This is in good consistency with the results published previously [7, 8]. Based on this observation, the pinning magnetic field was set at 900 Oe for further investigations.

Sensors with the same pinning magnetic field of H_{bias} = 900 Oe and the NiFe film of 5 nm thickness and with different length/width ratios were used to study the effect of the geometrical sensor configuration. The actual resistor bars
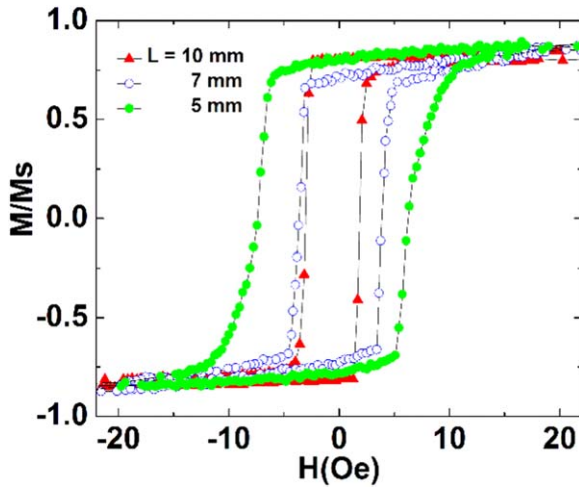
Figure 5. Magnetic hysteresis loops of sensors with the external magnetic field applied along the direction of the pinning magnetic field (H_{bias}).
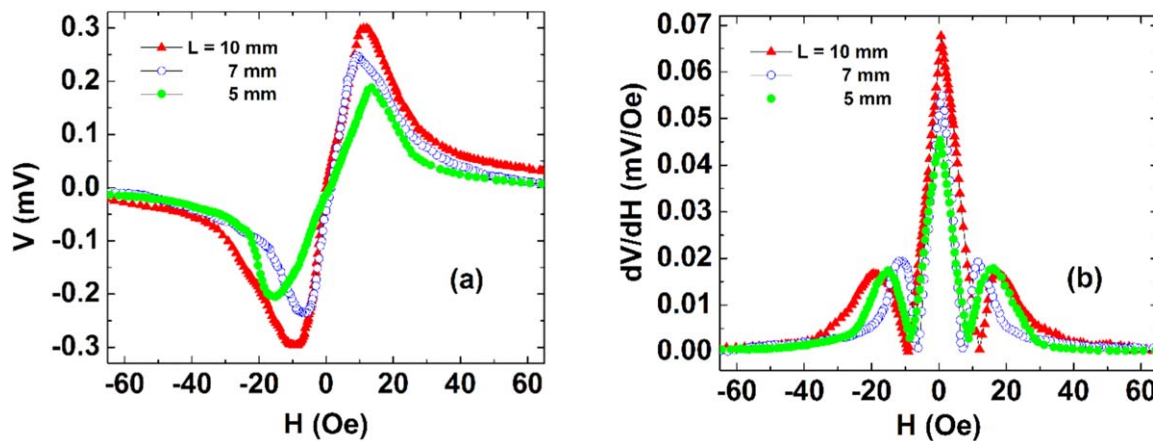
Table 1. The output voltage ΔV and the magnetic sensitivity $S_H = dV/dH$ for sensors of different sizes and thicknesses of sensors.

$W \times L \times t$ (mm×mm×nm)	ΔV (mV)	S_{H} (mV/Oe)	$S_{\text{H}}/I_{\text{in}}$ (mΩ/Oe)
$1 \times 5 \times 15$	0.38	0.045	9
$1 \times 7 \times 15$	0.50	0.055	11
$1 \times 10 \times 15$	0.60	0.07	14
$1 \times 10 \times 10$	0.74	0.08	16
$1 \times 10 \times 5$	0.90	0.10	20

of different sizes in width and length dimension as 1×5, 1×7, 1×10 mm^2 were fabricated. Magnetic hysteresis loops of these fabricated sensor configurations were taken with the applied field parallel to the H_{bias} and the results are presented in figure 5. As clearly seen from the recorded loops, the magnetic hysteresis decreases and the slope of these curves increases with the increasing length, e.g. the length/ width ratio of the sensors. It is clear that the anisotropic shape of the sensor has significantly contributed to the enhancement of its uniaxial anisotropy. It is also clear to see that the sensor of the size of 1×10 mm^2 exhibits the best soft magnetic properties with the smallest coercivity (in the order of approximately 2 Oe, only). This results in an enhanced sensitivity according to equation (3) above, from which we obtain the highest sensitivity for the lowest H_K field value that corresponds to the largest length to width ratio. It is also expected that this sensor will provide such a sensitivity high enough to be appropriately used for the detection and measurement of low and very low magnetic fields.

3.2. Planar Hall effect signal of sensors

For the further study on the PHE performance, sensors with different sizes 1×5, 1×7 and 1×10 mm^2 and the same NiFe thickness of 15 nm were used and the output Hall voltage, e.g. the planar Hall signal was measured in external magnetic fields. The Hall voltage was recorded while a current of $I_{\text{in}} = 5$ mA was sent through the sensor in the direction perpendicular to the sensor easy axis, which is parallel to the applied external magnetic field (refer to figure 2(c) above). The results of this measurement in terms of $V(H)$ are presented in figure 6(a). From this figure, it is clearly seen that the sensors with greater length to width ratio of the resistor bars deliver greater output signals. Indeed, a larger maximum Hall voltage $\Delta V_{\text{max}} = 0.6$ mV was found in the sensor with length/width ratio of 10, which is 1.6 times greater than 0.38 mV of the sensor with ratio of 5. In addition, the sensitivity of the sensor's output voltage to the external magnetic field $S_H^V = dV/dH$ extracted from the slope of the $V(H)$ curve is shown in figure 6(b). From the S_H^V, the sensitivity of the sensor's resistance to the external magnetic field was also included by using $S_H^R = dV/(dH \cdot I_{in})$ (see also in table 1). The plots also show that the sensitivity of the sensor with the length/width (L/W) ratio of 10 $(S_H^V = 0.07$ mV/Oe, $S_H^R = 14$ mΩ/Oe) is about 1.5 times greater than that of the sensor with length/width ratio of 5 $(S_H^V = 0.045$ mV/Oe, $S_H^R = 9$ $m\Omega$/Oe). This is due to the enhanced magnetic properties associated with the enhancement of the shape-anisotropy described above and it is also consistent with the

Figure 6. The output voltage (a) and the magnetic sensitivity (b) of sensors with different length/width ratios of 5, 7 and 10.
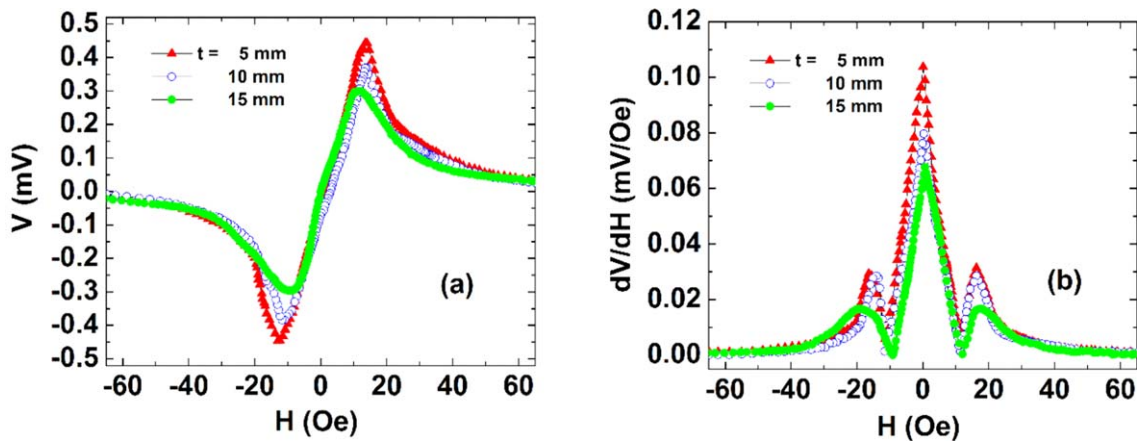
Figure 7. The output voltage (a) and the magnetic sensitivity (b) of sensors with different NiFe thicknesses of $t = 5, 10, 15$ nm.
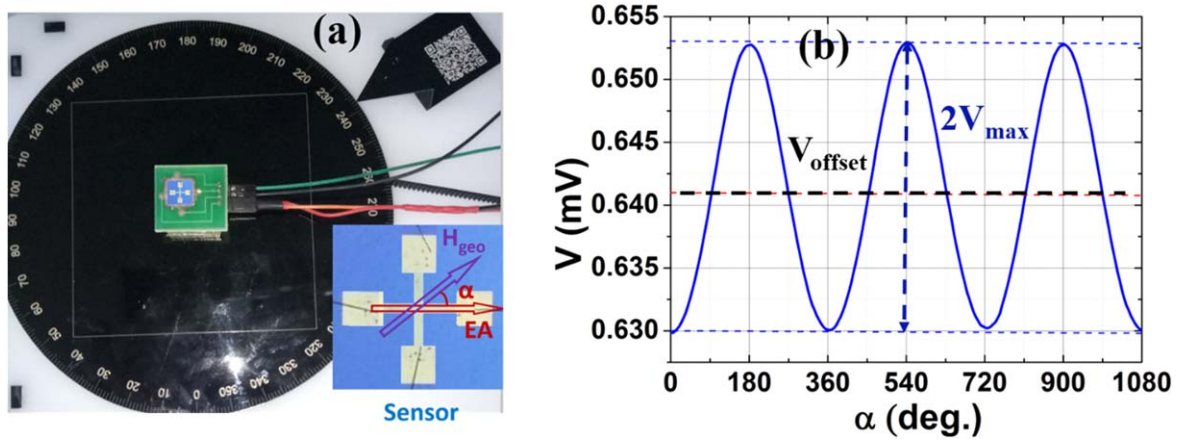
Figure 8. Experimental setup for Earth's magnetic field measurement (a), the output signal as a function of the α-angle between the sensor's longitudinal axis and the Earth's North Magnetic Pole (b).

observation of the sensor anisotropy shape effect shown previously [8].

For optimizing the thickness of NiFe layers, three 1×10 mm^2 sensors of different NiFe thicknesses of 5, 10 and 15 nm were fabricated. The output Hall voltage was measured at a current 5 mA directed perpendicularly to the sensor axis and parallel to the external magnetic field. The results are shown in figure 7 and the calculated data are listed in table 1. It can be seen in the figure that the output voltage signals respond linearly to the applied magnetic field in the field region less than 10 Oe. The thinner the NiFe resistor bar, the better performance of the sensor with respects to both the output voltage signal and the magnetic field sensitivity. The highest output voltage signal and magnetic field sensitivity of $\Delta V = 0.9$ mV and $S_H = 0.1$ mV Oe^{-1}, respectively, corresponding to relative resistance change up to 20 mΩ/Oe were achieved by the sensor with the NiFe film thickness of 5 nm which are higher (by 1.5 and 1.4 times, respectively) than those obtained on the sensors with the NiFe layer thickness of 10 and 15 nm. This can also be attributed to the strengthening of the uniaxial magnetic anisotropy thanks to the in-plane shape magnetic anisotropy enhancement of the resistor bar. The effect also shows the same tendency as observed on the sensor with different sizes and geometrical

configurations shown above. These results are consistent with those in previous works on the AMR effect in the Wheatstone bridge sensor using the same resistor materials of our group [8] and in good agreement with the results reported by Mor *et al* [23].

The results discussed above have revealed that sensors with a thinner NiFe layer and a higher length/width ratio of the resistor bars exhibit better low magnetic field sensing performance. The sensor optimum dimension would be 1×10 mm^2 in size and 5 nm in thickness that possesses a sensitivity as high as 100 μV/Oe (20 mΩ/Oe). This value is 10.5, 6.4 and 5 times, respectively, higher than those reported in the previous literatures on the cross-shaped Hall sensor using NiFe/IrMn ($S_H^V = 9.5$ μV/Oe) [12], NiFe/Cu/NiFe/IrMn ($S_H^V = 15.6$ μV/Oe) [4] and NiFe/Cu/NiFe/IrMn ($S_H^V = 19.86$ μV/Oe) [16], and comparable with the greatest result on Wheatstone bridge sensor published by Henriksen (sensitivity of 150 μV/Oe [2], 54.5 mΩ/Oe [14]). In comparison with our recent reports on AMR Wheatstone bridge sensors [7, 8, 22], this sensitivity is 10 times lower. On the other hand, compared to our previous AMR sensor with a sensitivity of 0.55 mV Oe^{-1} that has a detection limit of magnetic moments estimated to be about 0.56 μemu [22], the PHE sensor in this work can detect at a limit of about

3.1 μemu. It is also noteworthy that this sensitivity is one order of magnitude better than 10^{-5} emu, reported previously by Volmer [18]. The advantage of this cross-shaped Hall sensor is indeed the perfectly linear response in a low magnetic field range without any bias working field that could not be achieved with the AMR, TMR, GMR, valve-spin sensors [3, 4, 6, 7, 10–12, 14, 18, 19, 24].

3.3. Application for the Azimuth angle measurement of Earth's magnetic field

The sensor with 1×10 mm^2 in size and 5 nm in thickness was used to measure the Azimuth angle (α-angle) of Earth's magnetic field (H_{geo}). The experimental setup using the sensor is shown in figure 8(a) and the Azimuth angle dependence of the sensor's output voltage is plotted in figure 8(b). In this measurement, the sensor was placed in the horizontal plane and the Azimuth is defined as the angle between the H_{geo} direction and the sensor's easy axis (see the inset in figure 8(a)). A DC current of 5 mA was supplied for this measurement. The output voltage was perfectly fitted with a function:

$$V = V_{offset} + V_{max} \cos \alpha \, (mV), \qquad (4)$$

from which, the values of $V_{offset} = 0.641$ mV and $V_{max} = 0.012$ mV were estimated. From the highest slope, the sensitivity for Azimuth angle detection is estimated as about 0.4 μV/degree. Thanks to the relatively high sensitivity and the simple fabrication procedure, this sensor is promising for navigation application, such as in E-compass.

4. Conclusions

With a simple fabrication procedure, an efficient sensor based on PHE was made for the measurement of low magnetic fields. By optimizing the technological procedure and the structures of the sensor, enhanced PHE was achieved, thereby increasing the sensor's output signal and thus improving the sensor's sensitivity. An efficient sensor with the size of 1×10 mm^2, using NiFe thin film with a thickness of 5 nm was developed reaching a sensor's maximal output signal of $\Delta V = 0.9$ mV and thus a sensor's sensitivity of $S_H^V = 0.1$ mV/Oe (20 mΩ/Oe). The sensor was used to examine the Earth's magnetic field using the function $V = V_{offset} + V_{max} \cos\alpha$ (mV) with fitting parameters $V_{offset} = 0.641$ mV and $V_{max} = 0.012$ mV. This suggests the sensor to be a promising candidate for low field magnetic field sensing in biomedical applications.

Acknowledgments

References

[1] Bui D T, Tran Q H, Nguyen T T, Tran M D, Nguyen H D and Kim C G 2008 *J. Appl. Phys.* **104** 074701

[2] Henriksen A D, Dalslet B T, Skieller D H, Lee K H, Okkels F and Hansena M F 2010 *J. Appl. Phys. Lett.* **97** 013507

[3] Brajalal S, Tran Q H, Torati S R, Sunjong O, Kim K, Kim D-Y, Ferial T and Kim C G 2013 *J. Appl. Phys.* **113** 063903

[4] Bui D T, Le V C, Tran Q H, Do T H G, Tran M D, Nguyen H D and Kim C G 2009 *IEEE Transactions on Magnetics* **45** 2378

[5] Chenying W, Jiangtao P, Zhongqiang H, Wei S, Mengmeng G, Bin P, Ziyao Z, Zhiguang W, Zhuangde J and Ming L 2019 *IEEE Transactions on Magnetics* **55** 2501103

[6] Baselt D R, Lee G U, Natesan M, Metzger S W, Sheehan P E and Colton R J 1998 *Biosens. Bioelec.* **13** 731

[7] Hien L T, Quynh L K, Huyen V T, Tu B D, Hien N T, Phuong D M, Nhung P H, Giang D T H and Duc N H 2016 *Adv. in Nat. Sci. Nanosci. Nanotech.* **7** 045006

[8] Quynh L K, Tu B D, Dang D X, Viet D Q, Hien L T, Giang D T H and Duc N H 2016 *J. Sci. Adv. Mat. and Dev.* **1** 98

[9] Haji-Sheikh M J and Yoo Y 2007 *Inter. J. of Intelligent Sys. Tech. Appl.* **3** 95

[10] Richard G, Muthuvel M R, Sanjay S and Robert G 2004 *IEEE Sensors Journal* **4** 764

[11] Hung T Q, Oh S J, Tu B D, Duc N H, Phong L V, Kumar S A, Jeong J-R and Kim C G 2009 *IEEE Trans. Mag.* **45** 2374

[12] Tran Q H, Jong-Ryul J, Kim D-Y, Duc N H and Kim C G 2009 *J.Phys. D: Appl. Phys.* **42** 055007

[13] Van S L, Anh T N, Quoc K H, Tuyet N N, Anh T N, Tuan A N and Van C G 2018 *J. Sci. Adv. Mat. and Dev.* **3** 399–405

[14] Henriksen A D, Giovanni R and Mikkel F H 2016 *J. Appl. phys.* **119** 093910

[15] Nguyen V D F, Schuhl A, Childress J R and Sussiau M 1996 *Sens. Actuators* A **53** 256

[16] Kim H, Reddy V, Kim K W, Jeong I, Hu X H and Kim C G 2014 *Journal of Magnetics* **19** 10

[17] Hong Q P, Bang V T, Duy T D, Van S L, Quang N P, Kim K, Kim C G, Ferial T and Quang H T 2018 *IEEE Transactions on Magnetics* **54** 6201105

[18] Marius V and Marioara A 2015 *J. Mag. Mag. Mat.* **381** 481

[19] Giang D T H, Duc P A, Ngoc N T and Duc N H 2012 *Sens. Actuators* A **179** 78

[20] Giang D T H, Duc P A, Ngoc N T, Hien N T and Duc N H 2012 *Journal of Magnetics* **17** 308

[21] Vytautas M, Dangirutis N, Adam I, Darius A, Algimantas V and Mindaugas Z 2018 *Sensors* **18** 2225

[22] Quynh L K, Tu B D, Anh C V, Duc N H, Phung A T, Dung T T and Giang D T H 2019 *J. Electronic Materials* **48** 997

[23] Mor V, Schultz M, Sinwani O, Grosz A, Paperno E and Klein L 2012 *J. Appl. Phys.* **111** 07E519

[24] Yan S, Zhiqiang C, Zongxia G, Zhenyi Z, Anni C, Yue Q, Qunwen L and Weisheng Z 2018 *Sensors* **18** 1832